Marine and Petroleum Geology xxx (2015) 1–11

Contents lists available at ScienceDirect

Marine and Petroleum Geology

journal homepage: www.elsevier.com/locate/marpetgeo

Research paper

Formation of magnetic minerals at hydrocarbon-generation conditions

R. Abubakar [a, *], A.R. Muxworthy [a], M.A. Sephton [a], P. Southern [b], J.S. Watson [a], A.J. Fraser [a], T.P. Almeida [a]

[a] Department of Earth Science and Engineering, Royal School of Mines, Imperial College London, South Kensington Campus, London SW7 2AZ, UK
[b] University College London Healthcare Biomagnetics and Nanomaterials Laboratories, 21 Albemarle Street, London W1S 4BS, UK

ARTICLE INFO

Article history:
Received 30 December 2014
Received in revised form
24 August 2015
Accepted 2 October 2015
Available online xxx

Keywords:
Pyrolysis
Petroleum generation
Magnetism
Oil exploration

ABSTRACT

In this paper, we report the pyrolysis and formation of magnetic minerals in three source rock samples from the Wessex Basin in Dorset, southern England. The experimental conditions in the laboratory recreated the catagenesis environment of oil source rocks. Magnetic analysis of both the heated and the unheated samples at room temperature and at very low-temperatures (5 K), coupled with transmission electron-microscopy imaging and X-ray analysis, revealed the formation of nanometre-sized (<10 nm), magnetic particles that varied across the rock samples analysed, but more importantly across the pyrolysis temperature range. Magnetic measurements demonstrated the formation of these magnetic minerals peaked at 250 °C for all rock samples and then decreased at 300 °C before rising again at 320 °C. The newly formed magnetic minerals are suggested to be primarily pyrrhotite, though magnetite and greigite are also thought to be present. The sizes of the magnetic minerals formed suggest a propensity to migrate together with oil potentially explaining the magnetic anomalies observed above and within oil fields.

1. Introduction

A number of studies of near-surface soil samples from oil fields (Díaz et al., 2000; Aldana et al., 2003; Costanzo-Alvarez et al., 2006; Emmerton et al., 2013) have revealed the presence of authigenic magnetite, whereas similar studies on near surface soil samples from areas with no known hydrocarbon accumulations do not reveal the presence of magnetite. The formation of magnetic minerals in sedimentary columns has been linked to the action of heat due to burial (Lu et al., 1990; Katz et al., 2000; Cairanne et al., 2004; Moreau et al., 2005; Aubourg et al., 2008; Aubourg and Pozzi, 2010; Aubourg et al., 2012; Kars et al., 2012) and also to secondary processes that involve microbial reduction of Fe^{3+} to Fe^{2+} iron in the presence of hydrocarbons (Donovan et al., 1979; Díaz et al., 2000; Aldana et al., 2003; Emmerton et al., 2013). Magnetic techniques can detect these magnetic minerals and have been proposed as a complimentary tool for the exploration of oil and gas (Donovan et al., 1979; Burton et al., 1993; Leblanc and Morris, 1999; Costanzo-Alvarez et al., 2006).

In order to explain the origin of these magnetic minerals and their association with hydrocarbon reservoirs, two basic mechanisms have been proposed: (1) abiotic, and (2) microbial. Burton et al. (1993) developed an abiotic thermodynamic model explaining how the magnetic response of magnetic minerals could be both increased or decreased depending on the local chemical environment, e.g., sulphur rich or not, and proximity to hydrocarbon plumes. Other authors (e.g., Aldana et al., 2003; Costanzo-Alvarez et al., 2006) have also argued for abiotic formation mechanisms for magnetic mineral formation, but have also suggested that microbial action can be the cause of magnetic mineral formation in the presence of crude oils.

Abiotic processes have also been ascribed for the generation of magnetic minerals observed in sedimentary successions in general (McCabe et al., 1987; Ellwood and Crick, 1988; Lu et al., 1990; Bjorlykke, 1998; Katz et al., 2000; Cairanne et al., 2004; Moreau et al., 2005; Aubourg et al., 2008; Aubourg and Pozzi, 2010; Aubourg et al., 2012). Moreau et al. (2005), Aubourg and Pozzi (2010), Aubourg et al. (2012) amongst others, carried out an experimental investigation to study the action of heat (simulated burial, both at atmospheric pressure and under confined

* Corresponding author.
E-mail address: r.abubakar09@imperial.ac.uk (R. Abubakar).

http://dx.doi.org/10.1016/j.marpetgeo.2015.10.003
0264-8172/

pressure) on clay minerals by heating clay samples at 95–250 °C under various conditions (both exposed to air, and in liquids) in a magnetic field of 2 mT over various periods. Aubourg et al. (2012) reported how thermal/hydrothermal effects impart chemical remanent magnetisation (CRM) acquisition in rocks and the authors proposed a model which tries to explain magnetic mineral formations from early diagenesis to depths of about 10 km. Aubourg et al. (2012) showed transitional changes in magnetic mineral formations from greigite in sediments ~50 °C (equivalent to ≤ 2 km burial depth) to magnetite in the range ~50–200 °C (equivalent to ≤ 2–6 km burial depth) and to pyrrhotite for temperature > 200 °C (equivalent to > 6 km burial depth).

In this paper, we carried out hydrous pyrolysis experiments similar to Moreau et al. (2005) and Aubourg and Pozzi (2010), but in anoxic environments and under constant hydration in order to investigate the effects of petroleum generation on magnetic mineralogy in the laboratory and to have a better understanding of the stoichiometry, type, and abundance of magnetic minerals produced during the generation of oil and gas in the sub-surface. We subjected three potential source rocks from the Wessex Basin, UK, to laboratory conditions similar to those experienced during catagenesis by means of pyrolysis in pressure vessels for pressure control under anoxic conditions for 72 h at different temperatures. For pyrolysis temperatures 300 °C and 320 °C, the pressure was 80 and 100 bar respectively; at depth the pressures are significantly higher but in terms of petroleum generation, heat is the most critical factor (Pepper and Corvi, 1995; Helgeson et al., 2009; Stainforth, 2009). For example, at ~2 km depth, the temperature is typically ~50 °C with a pressure of ~150 bars, and at 6 km, the temperature is ~200 °C and the pressure ~600 bar. Source rocks that had experienced pyrolysis were then subjected to various magnetic analyses and the results were compared against unheated rocks. Transmission electron microscopy (TEM) combined with energy-dispersive X-ray (EDX) analysis of extracted magnetic minerals from the heated rocks was also carried out in an attempt to identify the magnetic minerals generated. Our findings will help to provide a better understanding of the nature of magnetic minerals formed during the generation and also as a result of the presence of oil in an environment and can help to interpret the often-problematical data generated by aeromagnetic surveys (e.g. Donovan et al., 1979; LeSchack and Van Alstine, 2002 and LeSchack and Jackson, 2003).

2. Methods

2.1. Oil source rock samples

Three oil source rocks were sampled from the Wessex Basin, UK: the Blue Lias, the Oxford Clay and the Kimmeridge Clay from Lyme Regis, Chickerell and Kimmeridge Bay respectively (Fig. 1). All are dark grey to black, fissile, marine shales containing Type II kerogen (Akande, 2012a). Kerogen has been defined as a polycondensate, partially soluble organic matter that is the end product of diagenesis of organic carbon (Tissot and Welte, 1984). The Oxford clay and Kimmeridgian samples are mature for oil generation, lying in the hanging wall of the Purbeck Fault (Hawkes et al., 1998). The Lias sample from Monmouth Beach in Lyme Regis is immature sitting on the footwall of the Abbotsbury-Ridgeway Fault. Each of the samples came from one rock from the locations described above. Rock-Eval data on samples from same locations showed an average total organic carbon (TOC) for Blue Lias, Kimmeridge and Oxford Clay of 8.%, 3.% and 3% respectively; temperatures of maximum hydrocarbon release by the rocks during Rock-Eval pyrolysis (T_{max}) of 417 °C, 428 °C and 423 °C respectively (Akande 2012a, b).

2.2. Hydrous pyrolysis

The surfaces of oil source rock samples were rinsed with dichloromethane (DCM) to remove any surface contamination. A 316 stainless steel pressure vessel was cleaned using DCM and methanol and allowed to dry. Thirty millilitres (30 ml) of deionized water was sonicated for 5 min to remove any dissolved gas and was added to the pressure vessel. 10 g of the powdered oil source rock sample was then added into vessel and the atmosphere purged with argon at 4 bar. The oven was set and the required temperature and the pressure within the vessel settled at around 100 bar after a couple of hours. After 72 h the oven was switched off, the vessel allowed 24 h to cool and the sample retrieved using a non-magnetic spatula. The pyrolysis temperatures used for this method were 250 °C and 320 °C.

More pyrolysis of the three rocks samples was carried out using an alternative method. Three millilitres of deionized water was put on a sonicator for five 5 min and then fed into borosilicate glass tubes. The glass tube end containing the water was immersed in liquid nitrogen until the water was frozen. A 10 mg sample of the rocks was then introduced into the glass tube and dipped into liquid nitrogen again until frozen. The open end of the tube was attached to an Edwards vacuum system and the tube atmosphere evacuated to 10^{-4} bar and then sealed using a torch. Three samples were prepared this way for each of the three rock samples. The vacuum sealed tubes containing the samples were then pyrolysed in a 316 stainless steel pressure vessel at 150 °C, 200 °C and 300 °C with a calculated amount of water in the vessel used to equalize pressures across the glass tube walls. The main advantage of the tube method was to allow the processing of multiple samples simultaneously at desired pyrolysis temperatures and also to rule out the possibility of any contamination coming from the steel-made pressure vessel. However, the two experiments are essentially the same as the amount of water required to ensure that samples in both types of experiments remain fully immersed in the liquid phase of the liquid–vapour system was carefully calculated. This is an important factor in hydrous pyrolysis. Throughout the experiments, pressure within the vessel was monitored via an external pressure gauge mounted on the vessel in order to avoid pressure/mass loss.

2.3. Magnetic measurements

Magnetic measurements were performed for both the original unheated material and the heated rocks at 5 K and at room temperature. The low-temperature and some of the room-temperature measurements were carried out at the Royal Institution of Great Britain, London, using a Quantum Design SQUID vibrating sample magnetometer (SQUID VSM). Two types of measurements were carried out using the SQUID VSM: zero-field cooled/field cooled (ZFC/FC) measurements and hysteresis measurements. The zero-field cooled (ZFC) measurements were carried out with the samples cooled down from room temperature (300 K) to 5 K in 10 K/minute steps in a zero magnetic field. At 5 K, the samples were induced with isothermal remanent magnetisation ($IRM_{7T@5K}$) of 7 T and the magnetic moment of the samples was measured as the samples were warmed to 300 K whereas during the field cooled (FC) measurements, samples were cooled from room temperature to 5 K in a field of 7 T, the field was removed at 5 K and the magnetic moments of the samples were measured as they were warmed to room temperature. RT-IRM_{7T} were also carried out on selected samples; the samples where induced with a field of 7 T at room temperature and their magnetic moments measured as they cool down to 20 K. The methods allow identification of certain low-temperature crystallographic transitions, small particles, and

Please cite this article in press as: Abubakar, R., et al., Formation of magnetic minerals at hydrocarbon-generation conditions, Marine and Petroleum Geology (2015), http://dx.doi.org/10.1016/j.marpetgeo.2015.10.003

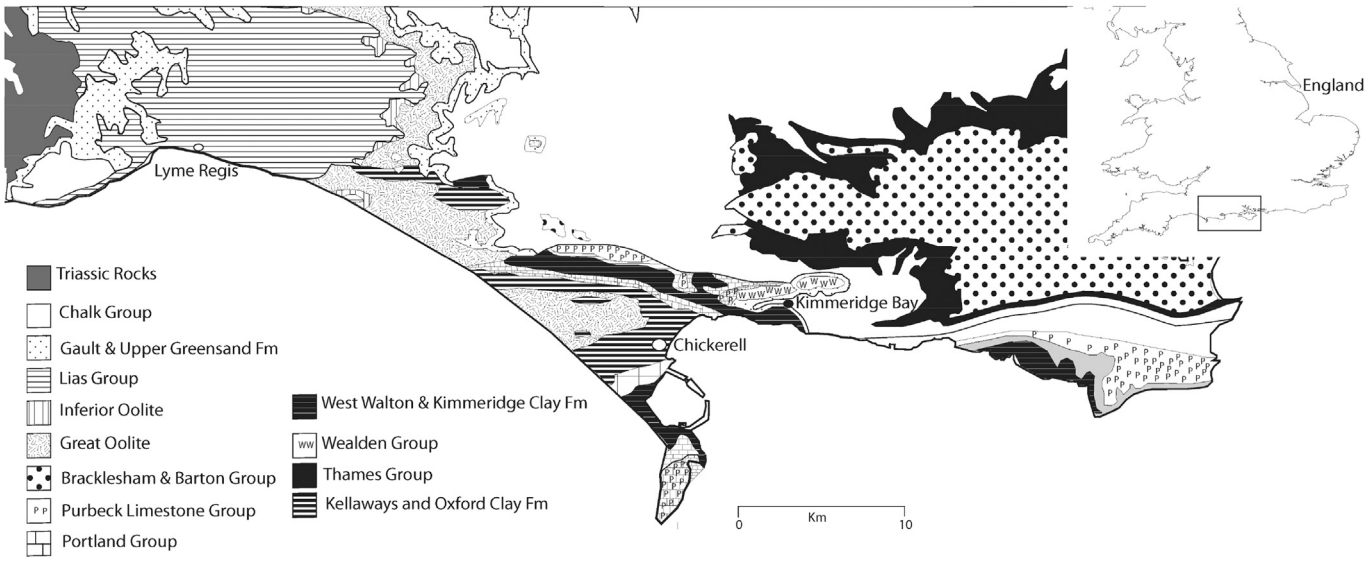

Fig. 1. Geological map of Wessex Basin showing sampling locations: Blue Lias (Lyme Regis), Oxford Clay (Chickerell), and Kimmeridge Clay (Kimmeridge Bay).

other minerals which are thermally activated (superparamagnetic) at room temperature. The second type of measurement using the SQUID VSM was hysteresis at 5 K and room temperature. For all three rock samples, the unheated rocks and the samples heated at 250 °C and 320 °C were measured using the SQUID VSM.

Room-temperature magnetic hysteresis measurements were made using a Princeton Measurements VSM located at Imperial College London, using a maximum field of 1 T. From the hysteresis measurements the standard hysteresis parameters were taken, i.e., the saturation magnetization M_s, the remanent saturation magnetization M_{rs} ($\equiv IRM_{1T@RT}$), the high-field susceptibility (χ_{hf}) and the coercive force B_c, and from the backfield curve the remanent coercive force B_{cr}. Thermomagnetic curves were measured using the Princeton VSM for Kimmeridge and Oxford Clays heated at 250 °C, 300 °C and 320 °C. Two types of measurements were carried out: 1) Single thermomagnetic experiments and 2) Multicycle thermomagnetic experiments. In the first type of the experiments, the rocks were heated to 700 °C and back to room temperature; in the second type the samples were heated to a given temperature and then back to room temperature, before heating to a higher temperature. The peak temperatures were 300 °C, 350 °C, 500 °C and 650 °C. In both experiments the samples were mixed with high-temperature cement and the heating was carried out in a stream of helium, giving rise to, if anything, a slightly reducing atmosphere. A magnetic field of 100 mT was applied.

2.4. Imaging

For the purpose of TEM, heated samples were run through a locally made magnetic extractor and extracted samples were dispersed in acetone using an ultrasonic bath before deposition onto lacey-carbon/copper-mesh support grids. Conventional bright field diffraction contrast and high-resolution phase contrast imaging was acquired using a FEI Tecnai TEM operated at 200 kV (Centre for Electron Nanoscopy (CEN), Technical University of Denmark) and selected area electron diffraction (SAED) allowed for phase identification. High-angle annular dark-field (HAADF) imaging and complementary EDX analysis were performed using a Jeol JEM 2100F TEM (Imperial College London). HAADF images were formed by collecting high-angle scattered electrons with an annular dark-field detector in scanning TEM (STEM) mode, where contrast is strongly dependent on the average atomic number (Z) of the sample encountered by the incident probe.

3. Results

3.1. Magnetic hysteresis

Room-temperature, magnetic hysteresis and backfield curves were measured on all the rock samples. The unheated samples all exhibited strong paramagnetic signals during hysteresis, with little or no evidence for a ferromagnetic (*sensu lato*) signal. That is, the three unheated samples have similar low-M_{rs} values (Table 1), though the Blue Lias sample has a stronger paramagnetic response; M_{rs} is direct measure of the amount of ferromagnetic material in a sample.

In contrast to the unheated samples the heated samples display significant ferromagnetic signals (Figs. 2–4). The shape of the hysteresis loops (not slope corrected) changed from predominantly paramagnetic to ferromagnetic in character and the intensity of the magnetisation increased significantly. For example, the unheated Kimmeridge Clay sample had a M_{rs} of 58 μA m^2/kg at room-temperature, but Kimmeridge Clay samples heated to 250 °C and 320 °C had M_{rs} values of 2510 μA m^2/kg and 8150 μA m^2/kg respectively, i.e., an order to two orders of magnitude increase in magnetic response. Similarly, there is a significant increase in the saturation magnetization (M_s) from 550 μA m^2/kg in unheated sample, to 6940 μA m^2/kg and 34,200 μA m^2/kg for Kimmeridge Clays heated at 250 °C and 320 °C respectively (Fig. 2 & Table 1). The Oxford Clay also shows a similar trend where samples heated at 250 °C and 320 °C had M_s values of 28,200 μA m^2/kg and 11,000 μA m^2/kg respectively against 560 μA m^2/kg for the immature sample, i.e., more than an order of magnitude increase with corresponding increase in the M_{rs} (Table 1).

In addition, a plot of M_s against pyrolysis temperature is shown in Fig. 3a. Compared to the unheated starting materials, all three rocks displayed clear increases in concentration of magnetic materials. Also supporting the evidence for the alteration of the ferromagnetic contribution to the hysteresis response is an increase in B_c; all the heated rocks had higher coercivities than their unheated counterparts save for Kimmeridge Clay 150 °C (Table 1 and Fig. 3b). The high-field magnetic susceptibility (χ_{hf}), which

Please cite this article in press as: Abubakar, R., et al., Formation of magnetic minerals at hydrocarbon-generation conditions, Marine and Petroleum Geology (2015), http://dx.doi.org/10.1016/j.marpetgeo.2015.10.003

Table 1
Room-temperature hysteresis parameters carried out on the three rock samples used in this study. χ = high-field susceptibility, B_{cr} = remanent coercivity, B_c = Coercivity, M_{rs} = saturation remanent magnetization, M_{rs}/M_s = ratio of saturation remanent magnetization to saturation magnetisation.

Sample	B_c (mT)	B_{cr} (mT)	B_{cr}/B_c	M_{rs} ($\mu Am^2/kg$)	M_s ($\mu Am^2/kg$)	M_{rs}/M_s	χ ($\times 10^{-7}$ m^3/kg)
Kimmeridge Clay immature	9.0	31	3.4	58	550	0.11	1
Kimmeridge Clay 150°	7.5	44	5.9	210	1530	0.14	0.50
Kimmeridge Clay 200 °C	16	35	2.2	240	1320	0.18	0.50
Kimmeridge Clay 250 °C	19	46	2.5	2510	6940	0.36	1
Kimmeridge Clay 300 °C	34	120	3.5	540	2300	0.23	0.50
Kimmeridge Clay 320 °C	11	25	2.4	8150	34,000	0.24	0.030
Oxford Clay immature	13	27	2.1	60	560	0.24	0.50
Oxford Clay 150 °C	13	47	3.5	140	660	0.21	0.50
Oxford Clay 200 °C	66	91	1.4	15,100	27,000	0.55	0. 60
Oxford Clay 250 °C	83	110	1.4	12,900	28,000	0.57	0.60
Oxford Clay 300 °C	35	–	–	620	2670	0.24	0. 50
Oxford Clay 320 °C	60	120	2.0	5030	11,000	0.46	0.02
Blue Lias immature	7.1	–	–	36	280	0.20	0.60
Blue Lias 150 °C	22	14	0.64	140	900	0.15	0.60
Blue Lias 200 °C	13	40	3.0	400	2980	0.11	0.60
Blue Lias 250 °C	11	27	2.4	180	980	0.19	0.00040
Blue Lias 300 °C	14	42	3.1	73	800	0.09	0.5
Blue Lias 320 °C	11	36	3.5	240	1380	0.17	−0.0010

measures the contribution of diamagnetic/paramagnetic material, varied across the three samples; all the heated Kimmeridge samples had lower χ_{hf} than the unheated sample except for Kimmeridge Clay heated at 250 °C with similar values to the unheated sample (Table 1). χ_{hf} values for the Oxford Clay and the Blue Lias were similar between the heated and the unheated samples (0.5–0.6 $\mu m^3/kg$) except for Oxford Clay and Kimmeridge Clay 320 °C which had lower values of about 0.002 $\mu m^3/kg$. The trend is similar in with Blue Lias 250 °C much less paramagnetic contribution (4×10^{-11}) and Blue Lias 320 °C having a diamagnetic contribution of -1×10^{-10}.

A few magnetic hysteresis measurements were also carried out at 5 K on the heated rocks. Oxford Clay (320 °C) measured at 5 K had a M_{rs} value of 21,400 $\mu A\ m^2/kg$ whereas the same sample measured at room temperature had a M_{rs} value of 5030 $\mu A\ m^2/kg$ (Table 1), representing about five times increase in magnetic remanence on cooling. The Blue Lias and Kimmeridge Clay samples also show similar trends in variation between magnetic measurements performed at room temperature and those carried out at 5 K.

3.2. Thermomagnetic curves

The single thermomagnetic run curves showed irreversibility on cooling from 600 to 700 °C with all the samples showing various amount of decay in moment from about 330 °C (Fig. 4 a–f insets) with the 250 °C and 320 °C samples (Fig. 4 c–f insets) exhibiting a secondary increase in magnetic moment above 400 °C. All the samples had a higher moment on cooling from 650 °C except for Oxford Clays 250 °C and 320 °C. Samples containing a mixture of magnetite and greigite will show an inflection at temperatures between 200 and 300 °C during thermomagnetic experiments if heating is carried out in a reducing atmosphere and the sample will

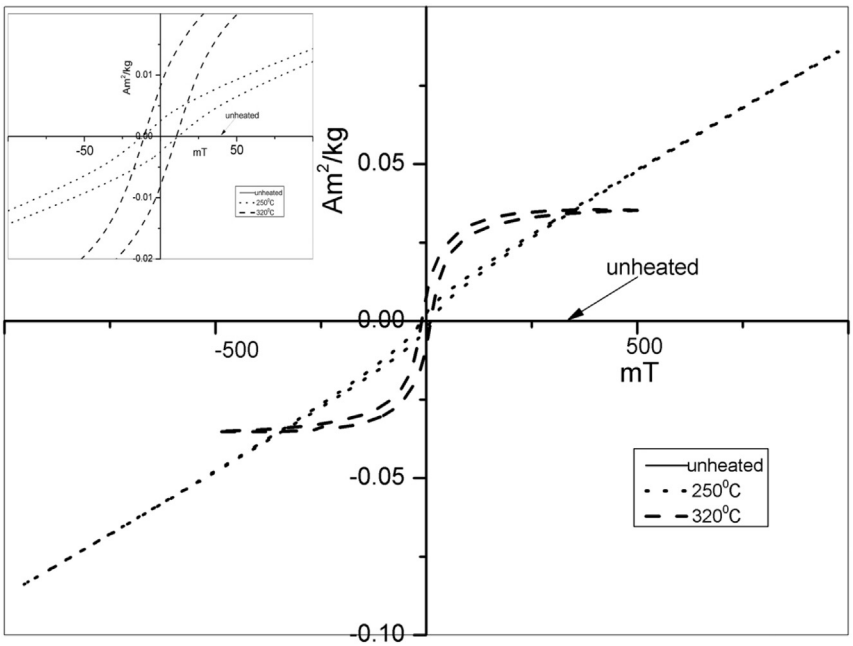

Fig. 2. Magnetic hysteresis plots for the Kimmeridge Clays immature and mature (320 °C & 250 °C) showing changes in magnetic response after heating. The immature sample response is almost flat and lies very close to the x-axis. The hysteresis loops do not have a paramagnetic correction.

Please cite this article in press as: Abubakar, R., et al., Formation of magnetic minerals at hydrocarbon-generation conditions, Marine and Petroleum Geology (2015), http://dx.doi.org/10.1016/j.marpetgeo.2015.10.003

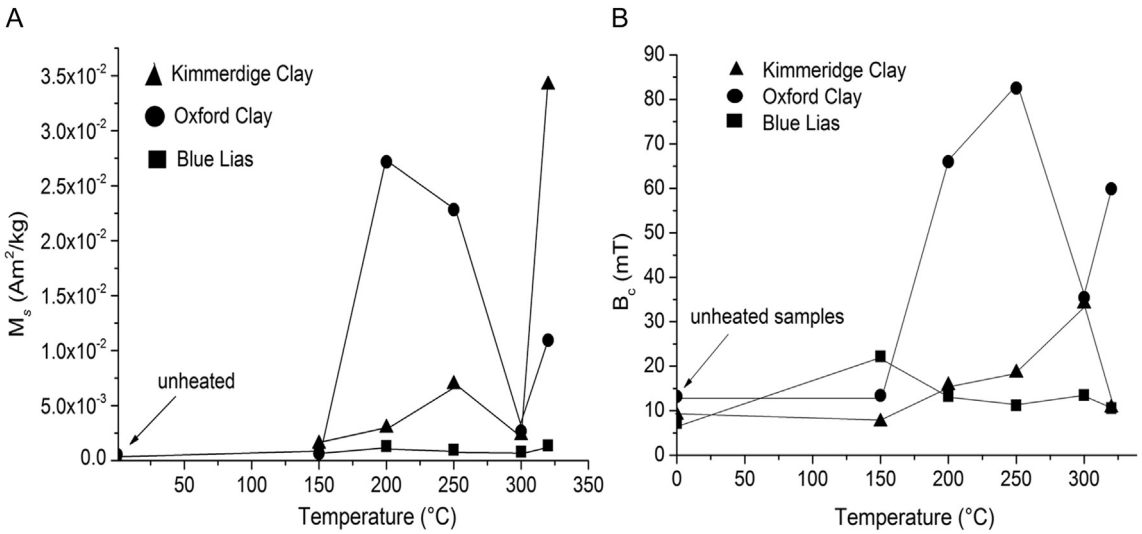

Fig. 3. A) A plot of saturation remanent magnetization (M_s) versus pyrolysis temperature. Oxford Clay showed a double peak M_s values first at 250 °C then a minimum at 300 °C and a secondary maximum at 320 °C. Kimmeridge Clay showed the highest Ms at 320 °C pyrolysis temperature. B) Plot of the magnetic coercivity (B_c) against pyrolysis temperature for all three source materials.

not show a marked minimum (Roberts et al., 2011). This behaviour was observed in Oxford Clay 320 °C (Fig. 4 f inset).

The multicycle thermomagnetic curves are mostly highly irreversible for the two rocks samples across the temperature ranges (Fig. 4). There is an increase of magnetic moment on cooling after heating to 300 °C in Oxford Clay 250 °C (Fig. 4b) but the Kimmeridge Clay 250 °C was nearly reversible on heating to the same temperature (Fig. 4b). There was a general increase in magnetic moment after the 350 °C cycle in Kimmeridge Clay (Fig. 4a) and a general decrease in moment after the 350 °C cycle Oxford Clay (Fig. 4b). The 300 °C and 350 °C cycles produced nearly reversible curves for both Kimmeridge and Oxford Clays 300 °C with a slight increase in magnetic moment on 350 °C cooling step (Fig. 4c and d) and a general increase in moment and similar behaviour between the two samples on the 500 °C and 650 °C cycles (Fig. 4e and f). Similarly, Kimmeridge and Oxford Clays 320 °C show similar trends, with an initial increase in moment on both 300 °C and 350 °C cycles and a significant drop in magnetic moment in the 500 °C and 650 °C steps.

3.3. Low-temperature warming and cooling curves

Two types of measurements were carried out here: 1) Warming curves of SIRMs induced at 5 K in a field of 7 T and warmed to room temperature shown in Fig. 5a–c. Two initial starting states were considered: after field-cooling (FC) from room temperature in a saturation field of 7 T and after zero-field cooling (ZFC) from room temperature. All the samples show a sharp drop in magnetization on heating, between 5 K and ~50 K, with a gradual decrease in magnetisation on warming ~50 K to room temperature. For all three samples the FC warming curves plotted above the ZFC data (Fig. 5a–c). During the warming experiments, initial magnetisation is seen to be much higher for the heated samples, compared to their unheated counterparts, providing further evidence for the production of magnetic minerals through pyrolysis. 2) Cooling curves of SIRMs at room temperature in a field of 7 T and cooled to 20 K was carried out on selected heated samples shown here in Fig. 5d. No crystallographic transitions were observed in any of the two experiments, suggesting that the demagnetisation observed on warming is due to the thermal relaxation of very small particles (~20–30 nm or finer) that are superparamagnetic at room temperature.

3.4. Transmission electron microscopy

We calculated mass concentration of magnetic minerals for all the three source rocks heated at 250 °C and 320 °C using the equation $f_{ferri} = Ms/\mu ferri$ (Lascu et al., 2010), where f_{ferri} is the mass fraction of the ferromagnetic component, M_s is saturation magnetization obtained from Table 1, μ_{ferri} is the ferromagnetic saturation magnetization with μ_{ferri} values for greigite, magnetite and pyrrhotite of ~59 A m^2/kg, 92 A m^2/kg and 17.2 A m^2/kg respectively (Dunlop and Özdemir, 1997; Chang et al., 2008). Mass concentration varies across the three rock samples with Blue Lias 250 °C and 320 °C having 11 and 15 ppm magnetite mass concentration respectively (Table 2), as a result we could not get enough material for imaging. However, Kimmeridge and Oxford Clays 320 °C had f_{ferri} magnetite mass concentrations of 371, 199 ppm respectively (Table 2) which was sufficient for extraction. TEM and EDX investigations provided high magnification imaging and chemical analysis of the magnetically extracted samples. Fig. 6 presents bright field TEM images of the magnetic extracts of the heated Kimmeridge Clay (320 °C). Large sheets are displayed in Fig. 6a and the associated selected area electron diffraction (SAED) pattern (inset) is in good agreement with that of Fe(II–III) hydroxysalt green rusts (GR1) (Almeida et al., 2012). The high magnification image of Fig. 6b presents a cluster of small particles (<20–30 nm in diameter) and the characteristic lattice fringes (inset) are consistent with the presence of Fe_3S_4, i.e., greigite. The HAADF image of Fig. 7a displays a group of GR1 sheets and the associated EDX chemical maps of Fig. 7b–h depicts the corresponding elemental distribution of Al, C, Fe, K, Mg, O and Si, respectively. Fig. 8 presents a high-angle annular dark-filed (HAADF) image (Fig. 8a) of an individual nanoparticle (~40 nm long, ~20 nm wide) and the associated EDX chemical maps show the elemental distribution of Fe (Fig. 8b) and O (Fig. 8c). The EDX spectrum of Fig. 8d displays the elemental constituents of the nanoparticle shown in Fig. 8a.

4. Discussion

All measurements carried out on the pyrolysed rock samples confirmed the formation ferromagnetic minerals. Although the three unheated samples had different amounts of magnetic

Please cite this article in press as: Abubakar, R., et al., Formation of magnetic minerals at hydrocarbon-generation conditions, Marine and Petroleum Geology (2015), http://dx.doi.org/10.1016/j.marpetgeo.2015.10.003

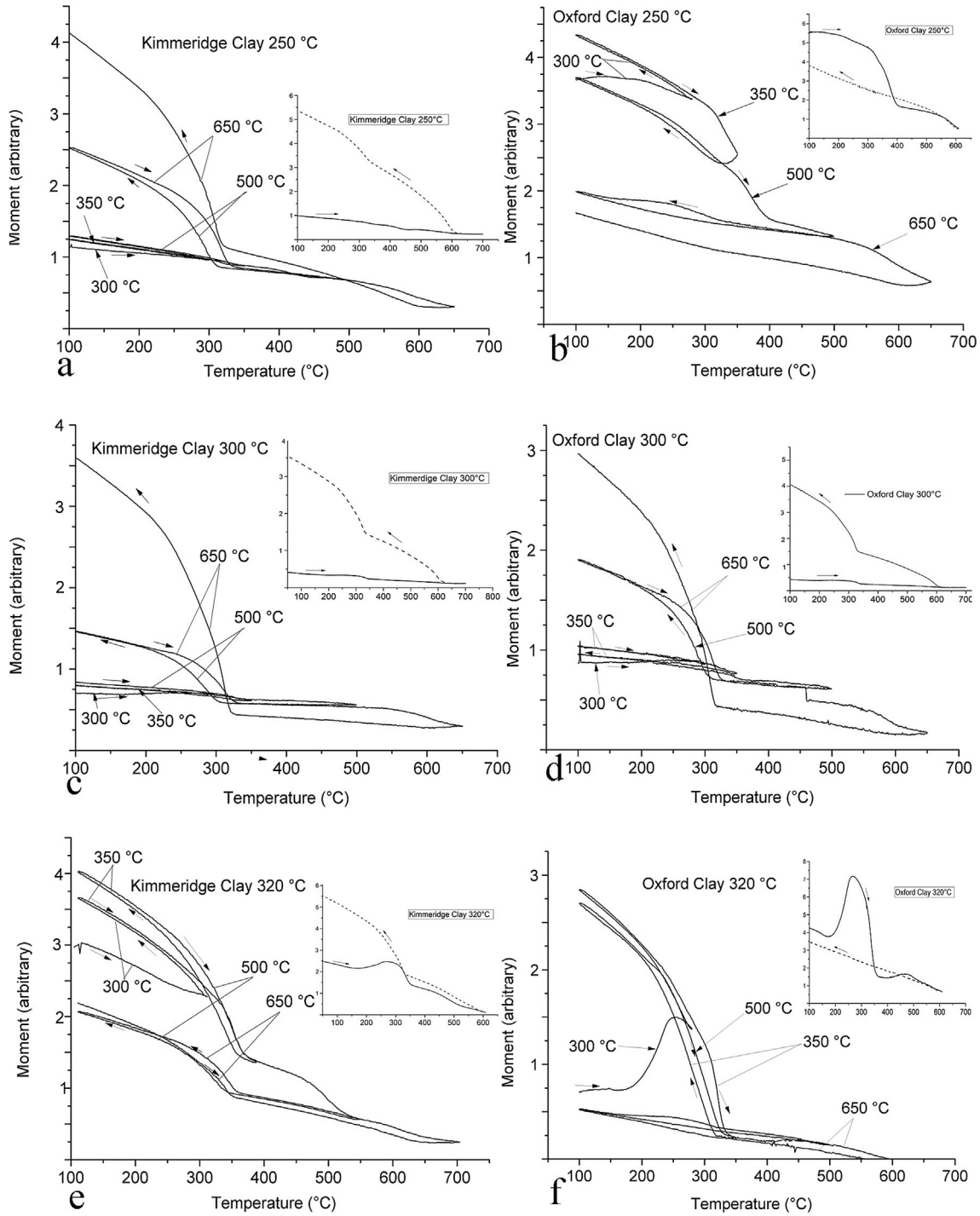

Fig. 4. Multicycle thermomagnetic curves showing slight alteration and increase in magnetic moment (a, c & d) that indicates possible alterations from greigite and/or to possible magnetite. Panels b e & f show an increase in moment after the first step, indicating alterations possibly to pyrrhotite and subsequent decrease in the moment in the 500 & 650 °C steps, indicating alterations to less magnetic mineral possibly pyrite and/or hematite. Insets: Continuous thermomagnetic curves indicating drop in magnetization on heating. (a, b, d & e) show drop of magnetization around 330 °C–400 °C which might indicate the presence of pyrrhotite and at around 600 °C which indicates the presence of magnetite. (c & f) indicate the presence of 'mixed' pyrrhotite due to the shape of the curve and magnetite. All heating was carried out on helium atmosphere.

minerals, upon heating they all displayed similar trends in magnetic mineral formation (Table 1). The Blue Lias had the weakest magnetic signal, presumably due to a smaller contribution of terrigenous material than the Oxford Clay and Kimmeridge Clay rocks (Deconinck et al., 2003). There is an increase in the amount of magnetic material in the heated samples based on the saturation magnetization values (Table 1), confirming the formation of magnetic minerals as reported in similar heating experiments (e.g. Aubourg and Pozzi, 2010; Aubourg et al., 2012 and Kars et al., 2012). Albeit it from a limited number of data points, two peaks of increase in M_s values were observed in all the three samples; a peak at pyrolysis temperature of 250 °C and another at pyrolysis temperature of 320 °C.

There was evidence of increase in magnetic grain sizes based on

Please cite this article in press as: Abubakar, R., et al., Formation of magnetic minerals at hydrocarbon-generation conditions, Marine and Petroleum Geology (2015), http://dx.doi.org/10.1016/j.marpetgeo.2015.10.003

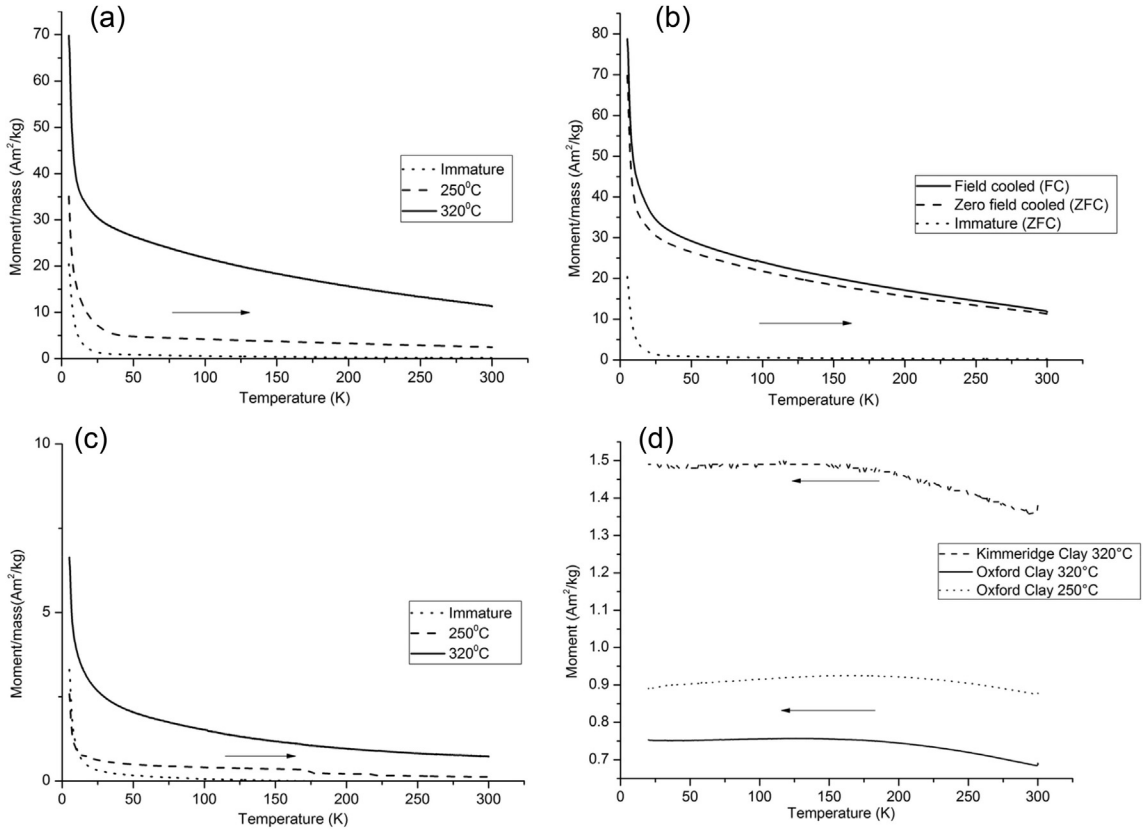

Fig. 5. Warming curves for the Kimmeridge Clay (a & b) and the Blue Lias (c) imparted with a saturation isothermal remanence in field of 7 T at 5 K. Two initial states are considered, zero-field cooling (ZFC) and (FC). ZFC samples were demagnetised at room-temperature before cooling in zero field to 5 K. FC samples were cooled in a field of 7 T from room-temperature to 5 K. Note the difference in scale of the magnetisation of both samples. (d) Shows RT-SIRM with no obvious drop in magnetization on cooling.

the saturation isothermal remanent magnetization (M_{rs}) values with double peaks also observed at 250 °C and 320 °C (Table 1). This double peak formation process is consistent with the model proposed by Aubourg et al. (2012) where they reported a peak for magnetite formation at about 200 °C to be gradually replaced by pyrrhotite until it is mainly pyrrhotite by about 300 °C. Also supporting the evidence of growth of magnetic grains is the overall increase in coercivities of the heated samples (Table 1). In addition, magnetic measurements carried out at 5 K showed larger magnetizations than at room temperature, e.g., for Kimmeridge Clay 250 °C $M_{rs} = 9450$ μA m^2/kg at 5 K compared with 2510 μA m^2/kg at room temperature. The Blue Lias 320 °C had $M_{rs} = 241$ μA m^2/kg at 300 K and 336 μA m^2/kg at 5 K, and the Oxford Clay 320 °C had $M_{rs} = 21{,}040$ μA m^2/kg at 5 K compared to $M_{rs} = 5030$ μA m^2/kg at room temperature. These indicate that the magnetic particles formed are ferromagnetic in nature but superparamagnetic at room temperature, i.e., small ferromagnetic particles are thermally unstable at room temperature and do not contribute to the ferromagnetic signal, but on cooling to 5 K become magnetically stable or 'blocked' and respond ferromagnetically (Nygård et al., 2004). However, some of the observed increases in magnetization could come from the contribution of Fe-bearing silicates, carbonates and sulphides, which can also become ferromagnetic or antiferromagnetic at very low-temperatures, i.e., <20 K.

Quantitatively, as a first approximation the blocking size of magnetite grain at room temperature is ~25 nm, but at 5 K is ~2 nm using data published in the literature (Dunlop, 1973) assuming a measurement time of 60 s. For greigite, under the same assumptions the value changes from ~18 nm at room temperature to ~5 nm at 5 K assuming that the magnetocrystalline anisotropy (−15 kJ/m^{-3} at room temperature) is temperature independent (Winklhofer et al., 2014).

Warming curves plotted to investigate the thermal relaxation of the magnetic particles in zero magnetic fields showed a sharp decrease in magnetization from about ~10 to 20 K for all the rock samples as they warmed to room-temperature (Fig. 5). This

Table 2
Mass concentration estimates (ppm) from hysteresis parameters for the three rock samples at different pyrolysis temperatures. Assumptions based on the presence of greigite, magnetite and pyrrhotite.

Sample	Magnetite (ppm)	Pyrrhotite (ppm)	Greigite (ppm)
Kimmeridge Clay 250 °C	75	403	1.18E-04
Kimmeridge Clay 320 °C	371	1990	5.79E-04
Oxford Clay 250 °C	248	1330	3.87E-04
Oxford Clay 320 °C	119	637	1.86E-04
Blue Lias 250 °C	11	57	1.66E-05
Blue Lias 320 °C	15	80	2.34E-05

Please cite this article in press as: Abubakar, R., et al., Formation of magnetic minerals at hydrocarbon-generation conditions, Marine and Petroleum Geology (2015), http://dx.doi.org/10.1016/j.marpetgeo.2015.10.003

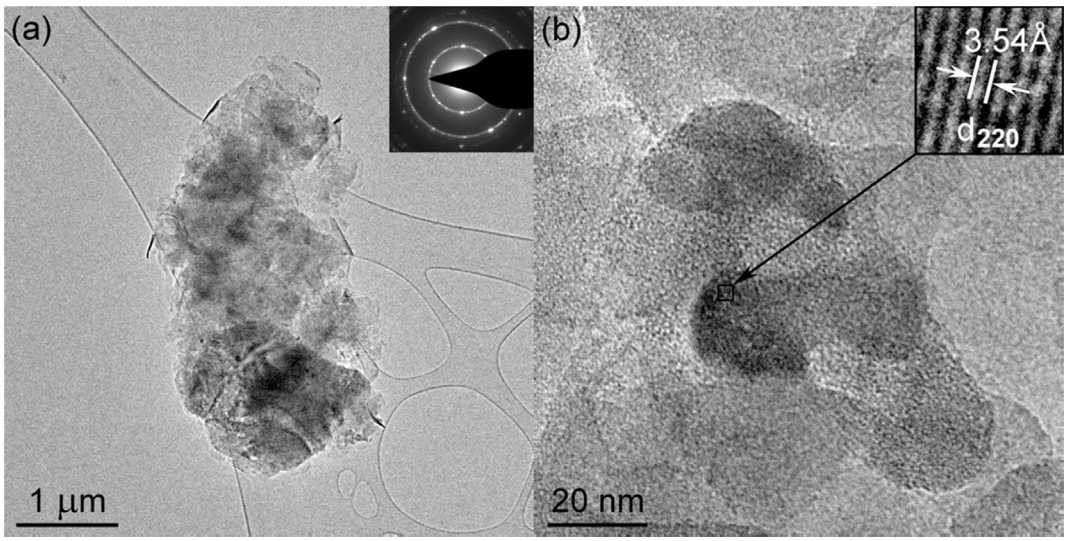

Fig. 6. Bright field TEM images of magnetic extract from Kimmeridge Clay (320 °C) showing (a) sheets of green rust, as identified by selected area electron diffraction (SAED) (inset); and (b) clusters of nanoparticles (<50 nm), with characteristic lattice fringes consistent with the presence of Fe_3S_4 (inset).

indicates that the magnetic enhancement is in very small particles <10 nm. The FC samples were slightly more magnetized than the ZFC samples (Fig. 5b) and the Blue Lias had a much lower magnetic remanence both during the FC and ZFC compared with the Oxford Clay and Kimmeridge Clay (Fig. 5c). No phase transitions were observed in the warming (Fig. 5a–c) and the RT-SIRM cooling curves (Fig. 5d), probably due to the sizes of magnetic grains present a being too small to exhibit low-temperature crystallographic transitions (Dekkers, 1989). TEM investigations showed that the extracted magnetic minerals are very small, less than <20–30 nm, and occur in clusters overlapping one another. This makes imaging of any single crystal problematic (Fig. 6). Complementary EDX analysis revealed strong signals from Fe (Fig. 8), thus confirming the presence of elemental constituents needed for the formation of magnetic minerals found within the magnetic extracts.

4.1. Magnetic mineralogy

Attempts were made using various techniques in order to identify the magnetic mineral present at various pyrolysis temperatures in our samples. The multicycle thermomagnetic measurements revealed the presence of sulphides in all the samples

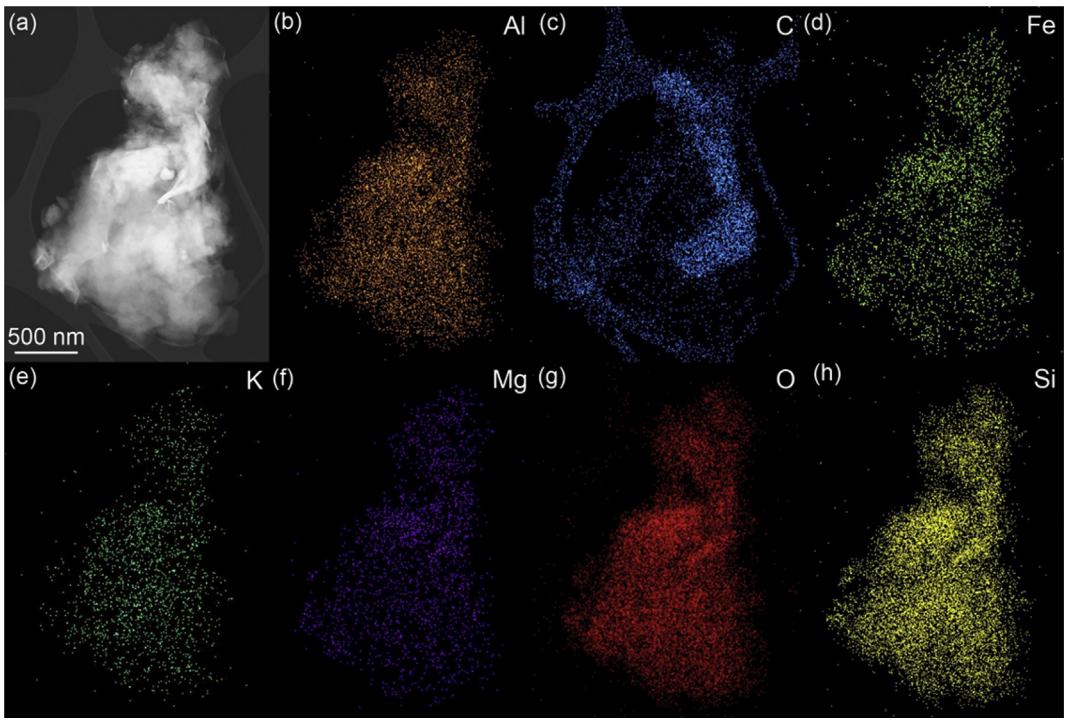

Fig. 7. (a) HAADF image of magnetic extract from Kimmeridge Clay (320 °C) showing sheets of green rust; and (b–h) EDX chemical maps showing (b) aluminium; (c) carbon; (d) iron; (e) potassium; (f) magnesium; (g) oxygen; and (h) silicon, content.

Please cite this article in press as: Abubakar, R., et al., Formation of magnetic minerals at hydrocarbon-generation conditions, Marine and Petroleum Geology (2015), http://dx.doi.org/10.1016/j.marpetgeo.2015.10.003

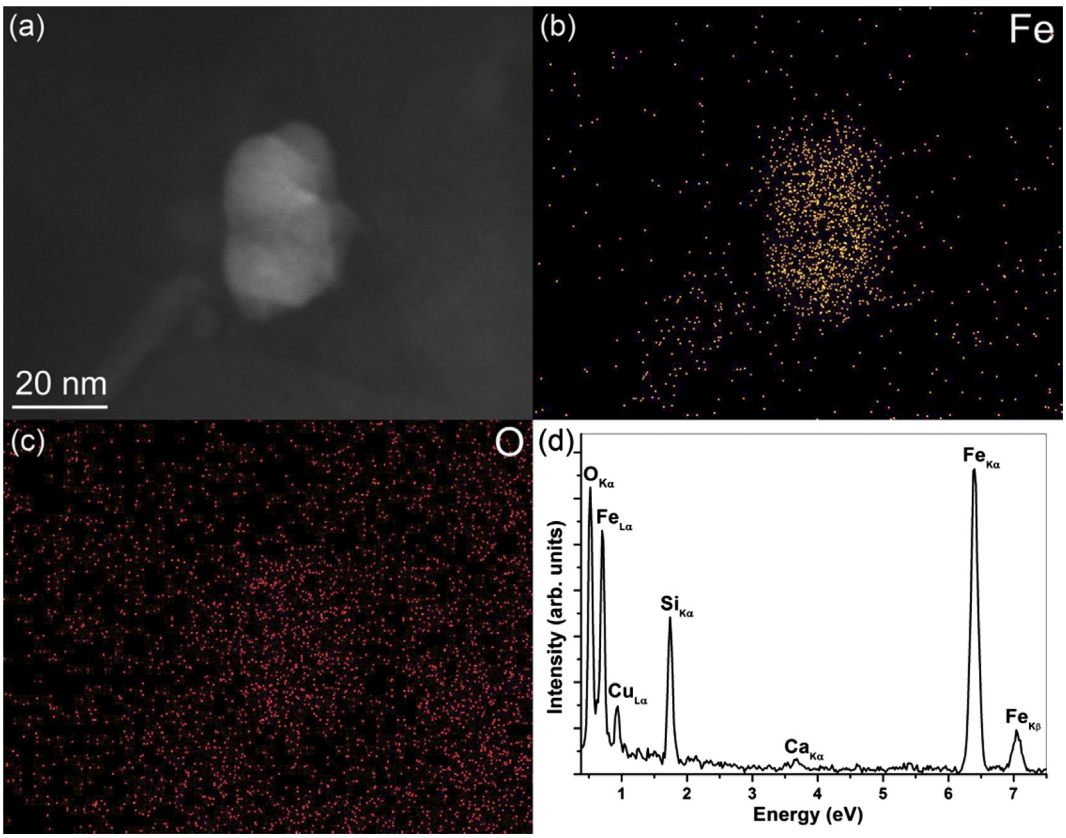

Fig. 8. (a) HAADF image of magnetic extract from Kimmeridge Clay (320 °C) showing an individual nanoparticle; and (b, c) EDX chemical maps showing (b) iron; and (c) oxygen, content. (d) EDX spectrum acquired from the centre of the particle shown in (a).

(Fig. 4). The Kimmeridge Clay 250 °C showed slight alterations during the initial thermomagnetic cycles, but a marked increase in moment after the 350 °C cycle which suggests a transformation of the sulphides present in the sample to possibly magnetite and/or the growth of pyrrhotite grains present in our samples (Fig. 4a) (Dekkers, 1990; Nilsson et al., 2013) and same behaviour was observed in both Kimmeridge and Oxford Clay 300 °C (Fig. 4 c and d). Conversely, Oxford Clay 250 °C showed an initial alteration to a more magnetic phase then a gradual decline in moment afterwards which suggests a partial alteration to pyrite after the 350 °C cycle and subsequently to hematite (Fig. 4b) (Dekkers, 1990). The structural transformations exhibited by all the samples at relatively lower temperatures of thermomagnetic experiments confirm the presence pyrrhotite and/or greigite in our samples (Torii et al., 1996).

The continuous thermomagnetic curves indicated the presence of both iron sulphides and magnetite in the samples (Fig. 4 insets): The peaks around ~300 °C are likely due to iron sulphide phases, i.e., monoclinic pyrrhotite, the Curie temperature near ~600 °C is indicative of magnetite. On cooling significant volumes of iron sulphide appear to have been generated suggesting the initial material was abundant in a non-magnetic iron sulphide, i.e., pyrite. Kimmeridge and Oxford Clays heated at 320 °C had a curve characteristic of an intergrowth of monoclinic and hexagonal (mixed) pyrrhotite (Fig. 4 c and f insets) as reported by Schwarz (1975). In addition, inflection observed in Oxford Clay 320 °C could suggest the presence of greigite (Roberts et al., 2011).

The absence of any low temperature crystallographic transition could also be because the dominant magnetic mineralogy present is either hexagonal pyrrhotite and/or greigite as they are reported not show low-temperature transitions with no definite Curie temperature (Roberts et al., 2011). The selection of greigite as a possible source may seem unusual as greigite is theoretically unstable to at room temperature and above (Aubourg and Pozzi, 2010; Aubourg et al., 2012), but Roberts et al. (2011) reported the occurrence of greigite hundreds – thousands of metres deep in sedimentary successions and argued greigite could occur as a stable mineral phase thousands of metres within sedimentary successions depending on oxygen fugacity, availability of organic matter and iron. . Greigite have also been reported to occur in heating experiments of temperatures in excess of 350 °C when heating is carried out in a reducing atmosphere (Dekkers et al., 2000). Furthermore, lattice fringes observed in the TEM were consistent with greigite (Fig. 6).

The drop in magnetisation observed in samples pyrolysed at 300 °C might be due to partial conversion of more magnetic minerals (greigite and magnetite) to pyrite. This is likely to occur under anoxic conditions (Karlin, 1990; Leslie et al., 1990).

Our findings agree with the with the theoretical thermodynamic models of Burton et al. (1993) who proposed that the formation of magnetic minerals due to burial is strongly influenced by proximity to hydrocarbon generation and accumulation, species of aqueous sulphur (HS^-, H_2S, or SO_4^{2-}) and bicarbonate (HCO_3^-), pH and Eh conditions. Aubourg and Pozzi (2010), Aubourg et al. (2012) proposed a conceptual model that tried to explain the chemical remanent magnetization (CRM) acquired during clay burial based on laboratory experiments conducted both at atmospheric pressures and at 100 MPa shielded from Earth's magnetic field with an applied vertical field of 2 mT and Kars et al. (2012) made an attempt to fully characterise the magnetic mineralogy, grain size or origin of

Please cite this article in press as: Abubakar, R., et al., Formation of magnetic minerals at hydrocarbon-generation conditions, Marine and Petroleum Geology (2015), http://dx.doi.org/10.1016/j.marpetgeo.2015.10.003

the CRM carriers in their study and they suggested that the process behind the neoformed CRM is relatively short in geological timescale. In our experiments, we produced crude oil at 320 °C by accelerating natural conditions and repeated same experiments at lower temperatures in order to fully investigate the applicability of magnetism as complimentary tool in the exploration of oil and gas as demonstrated by many authors (Leblanc and Morris, 1999; LeSchack and Van Alstine, 2002; Van Alstine and Butterworth, 2002; LeSchack and Jackson, 2003).

4.2. Implications for hydrocarbon research

We have established that magnetic minerals are abiotically and inorganically generated in conditions very similar to hydrocarbon generation conditions. In our experiments we accelerated the rate of reaction: In petroleum systems in general, the oil generation 'window' varies widely depending on the activation energies of organo facies present from ~95 to 135 °C and a gas generation window from ~135 to 155 °C, with heating rates varying ~0.5–2.0 °C Myr^{-1} (Pepper and Corvi, 1995); whereas in our experiments, we used a linear heating rate of 15 °C/minute which is far greater than what is observed under burial/heating conditions. It is problematic to accurately extrapolate our results to what is observable in geological records but there is a long track record of using high temperature and pressure reactors to simulate geological reactions on laboratory timescales (Lewan, 1993, 1998). The concept relies on the transformation rule in which the rate of chemical reaction is doubled for every 10 °C rise in temperature (Lewan, 1993; Pepper and Corvi, 1995; Lewan, 1998; Stainforth, 2009).

The abiotically generated magnetic particles are thought to be on average $\leq$ 10 nm, and have the potential to migrate along with crude oils since the sizes of pore-throats in sandstones range from 5 to 100 nm (Loucks et al., 2009; Nelson, 2009). Organic compounds found in crude oil reservoirs range from 4 to 100 nm in size (Loucks et al., 2009; Nelson, 2009) and assuming magnetic particles formed naturally are of similar sizes to those particles found in this study they could well migrate chelated to porphyrin molecules (through coordinate bonding) along with petroleum. Trace amount of metals have been discovered in crude oil samples from various regions (Shirey, 1931; Alberdi-Genolet and Tocco, 1999; Duyck et al., 2002) and some studies have tied these chelated metallic constituents to their source rocks using various ratios of Fe, Ni and V. These ratios were reported to be constant from source to crude oil samples analysed (Didyk et al., 1978; Sundararaman et al., 1993; Mudiaga et al., 2011).

5. Conclusions

This research has provided a better understanding of the formation of magnetic minerals in the subsurface through simulated burial and 'cooking' in the oil generation 'window'. We have shown that these processes produce significant – orders of magnitude greater – quantities of very small (<10 nm) ferromagnetic minerals, thought to be pyrrhotite and possibly magnetite. It is likely that at least part of the magnetic anomalies observed during aeromagnetic studies of oil fields (e.g., Donovan et al., 1979) or the magnetic minerals found in the studies of soil samples (Díaz et al., 2000; Costanzo-Alvarez et al., 2006; Emmerton et al., 2013) are formed via the same burial processes explored in this paper, i.e., they formed while petroleum is being generated thereby making it possible to use magnetism as a tool for oil and gas exploration.

Acknowledgements

This work was funded by the Petroleum Technology Development Fund (PTDF) Nigeria (PTDF/E/OSS/PHD/AR/381/11), the Natural Environment Research Council UK (NE/J01334X/1 & NE/H00534X/1) and the Centre for Electron Nanoscopy, Technical University of Denmark (NE/H00534X/1).

References

Akande, W.G., 2012a. Evaluation of hydrocarbon generation potential of the mesozoic organic-rich rocks using toc and rock-eval pyrolysis techniques. Geosciences 2, 6.
Akande, W.G., 2012b. Assessment of thermal maturity of the mesozoic organic-rich rocks of southern England. Pac. J. Sci. Technol. 13.
Alberdi-Genolet, M., Tocco, R., 1999. Trace metals and organic geochemistry of the Machiques member (Aptian–Albian) and la luna formation (Cenomanian–Campanian), Venezuela. Chem. Geol. 160, 19–38.
Aldana, M., Costanzo-Alvarez, V., Díaz, M., 2003. Magnetic and mineralogical studies to characterize oil reservoirs in Venezuela. Lead. Edge 22, 526–529.
Almeida, T.P., Fay, M., Zhu, Y., Brown, P.D., 2012. Controlling role of pH and temperature on $CoFe_2O_4$ nanostructures produced by hydrothermal synthesis. J. Nanosci. Nanotechnol. 12, 8801–8805.
Aubourg, C., Pozzi, J.-P., 2010. Toward a new <250 °C pyrrhotite–magnetite geothermometer for claystones. Earth Planet. Sci. Lett. 294, 47–57.
Aubourg, C., Pozzi, J.-P., Janots, D., Sarahoui, L., 2008. Imprinting chemical remanent magnetization in claystones at 95 °C. Earth Planet. Sci. Lett. 272, 9.
Aubourg, C., Pozzi, J.-P., Kars, M., 2012. Burial, Claystones Remagnetization and Some Consequences for Magnetostratigraphy. Geological Society, London. Special Publications 371.
Bjorlykke, K., 1998. Clay mineral diagenesis in sedimentary basins – a key to the prediction of rock properties. Examples from the North Sea Basin. Clay Miner. 33, 15–34.
Burton, E.A., Machel, H.G., Qi, J., 1993. Thermodynamic constrain on anomalous magnetization in shallow and deep hydrocarbon seepape environments. Soc. Sediment. Geol. 49, 15.
Cairanne, G., Aubourg, C., Pozzi, J.P., Moreau, M.G., Decamps, T., Marolleau, G., 2004. Laboratory chemical remanent magnetization in a natural claystone: a record of two magnetic polarities. Geophys. J. Int. 159, 909–916.
Chang, L., Roberts, A.P., Tang, Y., Rainford, B.D., Muxworthy, A.R., Chen, Q., 2008. Fundamental magnetic parameters from pure synthetic greigite (Fe_3S_4). J. Geophys. Res. Solid Earth 113 n/a–n/a.
Costanzo-Alvarez, V., Aldana, M., Bayona, G., Ayala, C., 2006. Hydrocarbon-induced magnetic contrasts in some Venezuelan and Columbian oil wells. Earth Planets Space 58, 10.
Deconinck, J.-F., Hesselbo, S., Debuisser, N., Averbuch, O., Baudin, F., Bessa, J., 2003. Environmental controls on clay mineralogy of an early Jurassic mudrock (blue lias formation, southern England). Int. J. Earth Sci. Geol. Rundsch) 92, 255–266.
Dekkers, M.J., 1989. Magnetic properties of natural pyrrhotite. II. High- and low-temperature behaviour of J_{rs} and TRM as function of grain size. Phys. Earth Planet. Interiors 57, 266–283.
Dekkers, M.J., 1990. Magnetic monitoring of pyrrhotite alteration during thermal demagnetization. Geophys. Res. Lett. 17, 779–782.
Dekkers, M.J., Passier, H.F., Schoonen, M.A.A., 2000. Magnetic properties of hydrothermally synthesized greigite (Fe_3S_4)—II. High- and low-temperature characteristics. Geophys. J. Int. 141, 809–819.
Díaz, M., Aldana, M., Costanzo-Alvarez, V., Silva, P., Pérez, A., 2000. EPR and magnetic susceptibility studies in well samples from some Venezuelan oil fields. Phys. Chem. Earth, Part A Solid Earth Geodesy 25, 447–453.
Didyk, B.M., Simoneit, B.R.T., Brassell, S.C., Eglinton, G., 1978. Organic geochemical indicators of palaeoenvironmental conditions of sedimentation. Nature 272, 216–222.
Donovan, T.J., Forgey, R.L., Roberts, A.A., 1979. Aeromagnetic detection of diagenetic magnetite over oil fields. AAPG Bull. 63, 245–248.
Dunlop, D.J., 1973. Superparamagnetic and single-domain threshold sizes in magnetite. J. Geophys. Res. 78, 1780–1793.
Dunlop, D.J., Özdemir, O., 1997. Rock magnetism. Fundamentals and frontiers. Cambridge studies in magnetism series. XXI + 573 pp. Cambridge, New York, Port Chester, Melbourne, Sydney: Cambridge University Press. Geol. Mag. 135, 287–300.
Duyck, C., Miekeley, N., Porto da Silveira, C.L., Szatmari, P., 2002. Trace element determination in crude oil and its fractions by inductively coupled plasma mass spectrometry using ultrasonic nebulization of toluene solutions. Spectrochim. Acta Part B At. Spectrosc. 57, 1979–1990.
Ellwood, B.B., Crick, R.E., 1988. Paleomagnetism of paleozoic asphaltic deposits in southern Oklahoma, USA. Geophys. Res. Lett. 15, 436–439.
Emmerton, S., Muxworthy, A.R., Sephton, M.A., Aldana, M., Costanzo-Alvarez, V., Bayona, G., Williams, W., 2013. Correlating biodegradation to magnetization in oil bearing sedimentary rocks. Geochim. Cosmochim. Acta 112, 146–165.
Hawkes, P.W., Fraser, A.J., Einchcomb, C.C.G., 1998. The tectono-stratigraphic development and exploration history of the Weald and Wessex Basins, Southern England, UK. Geol. Soc. Lond. Spec. Publ. 133, 39–65.
Helgeson, H.C., Richard, L., McKenzie, W.F., Norton, D.L., Schmitt, A., 2009. A chemical and thermodynamic model of oil generation in hydrocarbon source rocks. Geochim. Cosmochim. Acta 73, 594–695.
Karlin, R., 1990. Magnetite diagenesis in marine sediments from the oregon

Please cite this article in press as: Abubakar, R., et al., Formation of magnetic minerals at hydrocarbon-generation conditions, Marine and Petroleum Geology (2015), http://dx.doi.org/10.1016/j.marpetgeo.2015.10.003

continental margin. J. Geophys. Res. Solid Earth 95, 4405–4419.
Kars, M., Aubourg, C., Pozzi, J.-P., Janots, D., 2012. Continuous production of nano-sized magnetite through low grade burial. Geochem. Geophys. Geosystems 13, Q08Z48.
Katz, B., Elmore, R.D., Cogoini, M., Engel, M.H., Ferry, S., 2000. Associations between burial diagenesis of smectite, chemical remagnetization, and magnetite authigenesis in the Vocontian Trough, SE France. J. Geophys. Res. Solid Earth 105, 851–868.
Lascu, I., Banerjee, S.K., Berquó, T.S., 2010. Quantifying the concentration of ferrimagnetic particles in sediments using rock magnetic methods. Geochem. Geophys. Geosgystems 11. Q08Z19.
Leblanc, G.E., Morris, W.A., 1999. Aeromagnetics of Southern Alberta within areas of hydrocarbon accumulation. Bull. Can. Pet. Geol. 47, 439–454.
LeSchack, L.A., Jackson, J.R., 2003. Airborne Measurement of Transient Pulses Locates Hydrocarbon Reservoirs.
LeSchack, L.A., Van Alstine, D.R., 2002. High-resolution ground-magnetic (hrgm) and radiometric surveys for hydrocarbon exploration: six case histories in Western Canada. In: Schumacher, D., LeSchack, L.A. (Eds.), Surface Exploration Case Histories: Application of Geochemistry, Magnetics and Remote Sensing, AAPG in Geology, 48, pp. 67–156.
Leslie, B.W., Lund, S.P., Hammond, D.E., 1990. Rock magnetic evidence for the dissolution and authigenic growth of magnetic minerals within anoxic marine sediments of the California Continental Borderland. J. Geophys. Res. Solid Earth 95, 4437–4452.
Lewan, M.D., 1993. Laboratory simulation of petroleum formation. In: Engel, M., Macko, S. (Eds.), Organic Geochemistry. Springer, US, pp. 419–442.
Lewan, M.D., 1998. Sulphur-radical control on petroleum formation rates. Nature 391, 164–166.
Loucks, R.G., Reed, R.M., Ruppel, S.C., Jarvie, D.M., 2009. Morphology, genesis and distribution of nanometer-scale pores in siliceous mudstones of the Mississippian Barnett Shale. J. Sediment. Res. 79, 13.
Lu, G., Marshak, S., Kent, D.V., 1990. Characteristics of magnetic carriers responsible for late paleozoic remagnetization in carbonate strata of the mid-continent, U.S.A. Earth Planet. Sci. Lett. 99, 10.
McCabe, C., Sassen, R., Saffer, B., 1987. Occurrence of secondary magnetite within biodegraded oil. Geology 15, 7–10.
Moreau, M.G., Ader, M., Enkin, R.J., 2005. The magnetization of clay-rich rocks in sedimentary basins: low-temperature experimental formation of magnetic carriers in natural samples. Earth Planet. Sci. Lett. 230, 193–210.
Mudiaga, O.C., Oforka, N.C., Osuji, L.C., 2011. Trace metals geochemistry of crude oils from Umutu/Bomu fields in South West Niger delta Nigeria. EnergyEnviron. Res. 1, 7.
Nelson, P.H., 2009. Pore-throat sizes in sandstones, tight sandstones, and shales. AAPG Bull. 93, 329–340.
Nilsson, A., Lee, Y.S., Snowball, I., Hill, M., 2013. Magnetostratigraphic importance of secondary chemical remanent magnetizations carried by greigite (Fe_3S_4) in miocene sediments, New Jersey Shelf (iodp expedition 313). Geosphere 9, 510–520.
Nygård, R., Gutierrez, M., Høeg, K., Bjørlykke, K., 2004. Influence of burial history on microstructure and compaction behaviour of Kimmeridge clay. Pet. Geosci. 10, 259–270.
Pepper, A.S., Corvi, P.J., 1995. Simple kinetic models of petroleum formation. Part I: oil and gas generation from kerogen. Mar. Pet. Geol. 12, 291–319.
Roberts, A.P., Chang, L., Rowan, C.J., Horng, C.-S., Florindo, F., 2011. Magnetic properties of sedimentary greigite (Fe_3S_4): an update. Rev. Geophys. 49, RG1002.
Schwarz, E.J., 1975. Magnetic Properties of Pyrrhotite & their Use in Applied Geology & Geophysics. Geological Survey, Canada.
Shirey, W.B., 1931. Metallic constituents of cude petroleum. Ind. Eng. Chem. 23, 1151–1153.
Stainforth, J.G., 2009. Practical kinetic modeling of petroleum generation and expulsion. Mar. Pet. Geol. 26, 552–572.
Sundararaman, P., Raedeke, D.L., 1993. Vanadyl Porphyrins in Exploration: Maturity Indicators for Source Rocks and Oils. Elsevier, Kidlington, UK.
Tissot, B.P., Welte, D.H., 1984. Petroleum Formation and Occurrence. Springer-Verlag, Berlin; New York.
Torii, M., Fukuma, K., Horng, C.S., Lee, T.Q., 1996. Magnetic discrimination of pyrrhotite- and greigite-bearing sediment samples. Geophys. Res. Lett. 23, 1813–1816.
Van Alstine, D.R., Butterworth, J.E., 2002. Paleomagnetic Core Orietation Helps Determine the Sedimentological, Palestress and Fluid-migration History in the Maracaibo Basin. Congreso Virtual de Sedimentologia, Venezuela.
Winklhofer, M., Chang, L., Eder, S.H.K., 2014. On the magnetocrystalline anisotropy of greigite (Fe_3S_4). Geochem. Geophys. Geosystems 15, 1558–1579.

Please cite this article in press as: Abubakar, R., et al., Formation of magnetic minerals at hydrocarbon-generation conditions, Marine and Petroleum Geology (2015), http://dx.doi.org/10.1016/j.marpetgeo.2015.10.003